

# Far-UV Circular Dichroism Reveals a Conformational Switch in a Peptide Fragment from the $\beta$ -Sheet of Hen Lysozyme<sup>†</sup>

Jenny Jie Yang, Maureen Pitkeathly, and Sheena E. Radford\*

*Oxford Centre for Molecular Sciences and New Chemistry Laboratory, University of Oxford, South Parks Road, Oxford OX1 3QT, England*

*Received February 7, 1994; Revised Manuscript Received March 31, 1994\**

**ABSTRACT:** The conformation of a 20-residue synthetic peptide corresponding to the antiparallel triple-stranded  $\beta$ -sheet in hen egg white lysozyme (residues 41–60) has been studied by circular dichroism (CD) and size-exclusion chromatography. In aqueous solution the conformation of the peptide is strongly pH dependent. At pH values below 4.0 and 25 °C, the far-UV CD spectrum of the peptide resembles that expected for a predominantly  $\beta$ -sheet structure (low-pH form), while at pH values exceeding 4.0 the spectrum changes to that of a predominantly unstructured conformation (high-pH form). The far-UV CD spectrum of the high-pH form (pH 6.8) is not affected by changes in the concentration of the peptide and by changes in temperature and ionic strength. By contrast, the far-UV CD spectrum of the low-pH form (pH 2.0) is concentration and temperature dependent but is not affected by ionic strength. Size-exclusion chromatography has demonstrated that population of the low-pH state is associated with the formation of intermolecular trimers and higher oligomers and that the monomeric form of the peptide at low pH is predominantly random in nature. Significant helical structure was induced in the high-pH form of the peptide by both trifluoroethanol (TFE) and methanol; by contrast, the conformation of the low-pH form of the peptide was not changed with concentrations of methanol up to 50% (v/v), although in the presence of TFE a state displaying significant helical character was induced. During the transition an intermediate which also displays significant  $\beta$ -sheet character but which has a distinct CD spectrum is populated. The relevance of this study to the folding pathway of the intact protein is discussed.

An understanding of the driving force and the pathway(s) for the transformation of a polypeptide chain from a disordered, unfolded state into a compact and functional state has been actively pursued for many years. Although significant advances have recently been made in our understanding of the nature of stable partially folded states (Dobson, 1992; Haynie & Freire, 1993) and of the events in folding which occur on a millisecond to second time scale (Evans & Radford, 1994), the very earliest events which occur on a submillisecond time scale are still only poorly understood. To circumvent the extreme rapidity of these early events, peptide fragments corresponding to individual secondary structural elements, to domains, or to regions postulated to fold early have been studied (Dyson et al., 1992a,b; Cox et al., 1993; Shin et al., 1993), and the propensity of these peptides to adopt structure in aqueous solution has lent considerable support to the notion that secondary structural elements play an important role in the early events in protein folding.

The majority of studies on peptide fragments have focused on the conformational preferences of  $\alpha$ -helical peptides, such as the C-peptide from ribonuclease A (Brown & Klee, 1971; Shoemaker et al., 1987), the  $\alpha$ -helix of bovine pancreatic trypsin inhibitor (Goodman & Kim, 1989),  $\alpha$ -helical fragments of myoglobin (Shin et al., 1993), cytochrome *c* (Wu et al., 1993), and myohemerythrin (Dyson et al., 1992a), and "designed" synthetic sequences (Marqusee & Baldwin, 1987). Longer peptide sequences containing both  $\alpha$ -helical and  $\beta$ -sheet structures have also been examined (Oas & Kim, 1988),

although information related directly to the conformation of peptide fragments which adopt  $\beta$ -sheet structure in solution is relatively limited (Hilbich et al., 1991; Blanco et al., 1991; Dyson et al., 1992b; Fan et al., 1993) due to the tendency of these fragments to aggregate and, in general, their relatively low solubility (Hartman et al., 1974; Hilbich et al., 1991; Dyson et al., 1992b). Understanding the conformation of  $\beta$ -sheet structures is, however, of fundamental importance if we wish to dissect folding pathways, and aggregation of  $\beta$ -sheet structure is of major clinical interest since it has been implicated, for example, in amyloid deposition in Alzheimer's disease (Hilbich et al., 1991; Barrow et al., 1992; Terzi et al., 1994), and a single mutation in the  $\beta$ -sheet of human lysozyme has recently been shown to cause hereditary systemic amyloidosis (Pepys et al., 1993).

Theoretical calculations have suggested that the sheet-coil transition rate constant is about  $10 \text{ ns}^{-1}$  (Yapa et al., 1992). This is an order of magnitude slower than the helix-coil transition rate (McCammon et al., 1980); these relative rate constants open up the intriguing possibility, therefore, that  $\beta$ -sheet structures in intact proteins may form via  $\alpha$ -helical intermediates. Although there is little direct evidence that this is the case, it is of relevance in this regard that the intrinsic propensity of different amino acid sequences for distinct secondary structural elements is, in general, only weak, suggesting that peptide fragments in isolation may adopt different conformational states in different environments. For example, interconversion between  $\alpha$ -helical and  $\beta$ -sheet structures has been observed in peptide fragments of an ice nucleation protein (Ananthanarayanan et al., 1993) and of uteroglobin (Tessari et al., 1993), during the denaturation of monellin and ubiquitin by alcohols (Fan et al., 1993; Cox et al., 1993), and in the synthetic polymer poly(L-lysine) (Green-

<sup>†</sup> This paper is a contribution from the Oxford Centre for Molecular Sciences, which is supported by the SERC and MRC. S.E.R. is a Royal Society 1983 University Research Fellow.

\* To whom correspondence should be addressed.

\* Abstract published in *Advance ACS Abstracts*, May 15, 1994.

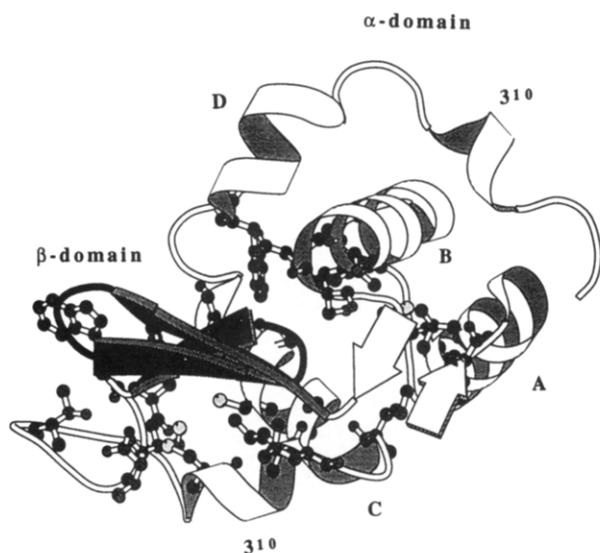


FIGURE 1: Native structure of hen lysozyme (Blake et al., 1965) emphasizing the location of the triple-stranded antiparallel  $\beta$ -sheet (residues 41–60). The side chains of 24 amino acids which lie within 4 Å of the  $\beta$ -sheet are shown. These include residues in helices A, B, C, and D and in the long loop in the  $\beta$ -domain. The figure was drawn using the program MolScript (Kraulis, 1991).

field & Fasman, 1969). In other cases, the propensity of a given sequence for a particular secondary structural element may be high. For example, peptide fragments corresponding to the  $\beta$ -sheet in the native state of *S*-3-trimethylated-amino propylated lysozyme (Segawa et al., 1991), in plastocyanin (Dyson et al., 1992b), and in the N-terminal  $\beta$ -hairpin in ubiquitin (Cox et al., 1993) do not adopt significant helical structure in aqueous solution or in the presence of alcohols, even though other regions in the lysozyme and ubiquitin sequences are able to adopt helical structure under these conditions (Segawa et al., 1991; Cox et al., 1993).

The folding of hen egg white lysozyme has been intensively studied in this laboratory by a variety of methods (Dobson et al., 1994). Hydrogen exchange labeling studies and 2D NMR<sup>1</sup> have revealed that the two lobes in the native structure are also distinct folding domains and that the folding pathway is complex and involves several alternative routes (Radford et al., 1992). In the majority of molecules, a major intermediate is populated in which the  $\alpha$ -helical domain folds to a persistent structure in the absence of a stable  $\beta$ -sheet domain. By contrast, there is no evidence to suggest that the  $\beta$ -sheet domain folds to a persistently structured state in advance of a stable  $\alpha$ -helical domain, at least in a substantial number of molecules (Miranker et al., 1993). Despite this, kinetic CD studies in the far-UV have suggested that a native-like complement of secondary structure is formed in the first few milliseconds of folding; these intermediates are not protected from hydrogen exchange, suggesting, therefore, that they are likely to have a high degree of fluctuating secondary structure (Chaffotte et al., 1992; Radford et al., 1992). In order to study the folding of the  $\beta$ -sheet domain in more detail, a peptide corresponding to the  $\beta$ -sheet of hen lysozyme (residues 41–60) (Figure 1) with the sequence  $\text{CH}_3\text{C}(\text{O})\text{-Gln-Ala-Thr-Asn-Arg-Asn-Thr-Asp-Gly-Ser-Thr-Asp-Tyr-Gly-Ile-Leu-}$

Gln-Ile-Asn-Ser-NH<sub>2</sub> has been synthesized, and the conformation of the peptide has been studied under a variety of conditions by far-UV CD.

## EXPERIMENTAL PROCEDURES

**Synthesis and Purification of the Peptide.** The  $\beta$ -sheet peptide was assembled on an Applied Biosystems 430A automated peptide synthesizer using the base-labile 9-fluorenylmethoxycarbonyl (Fmoc) group for the protection of the  $\alpha$ -amino function. Side-chain functional groups were protected by the *t*-Bu (Asp, Ser, Thr, Tyr), trityl (Asn, Gln), or Pmc (Arg) group. The peptide was assembled on the 4-(2',4'-dimethoxyphenyl-Fmoc-aminomethyl)phenoxy resin to produce a peptide with a C-terminal amide moiety (approx. 0.4 mmol g<sup>-1</sup>, 0.5 mmol, purchased from Novabiochem) using diisopropylcarbodiimide (DIC)/hydroxybenzotriazole (HOBt) mediated couplings (2 equiv each of amino acid, DIC, and HOBt) which were repeated twice for each residue. Capping of unreacted N-termini was carried out using a 1:1 mixture of acetic anhydride and pyridine in DMF. The Fmoc groups were cleaved by 20% piperidine in DMF, and cycles were modified to allow spectroscopic monitoring of aliquots of each deprotection mixture to allow the progress of synthesis to be monitored. The N-terminus of the peptide was acetylated on the synthesizer using a 4-fold excess of acetic anhydride and pyridine. The peptide-resin was treated with 85% TFA/5% H<sub>2</sub>O/5% ethanedithiol/5% thioanisole at room temperature for 1.5 h. The resin was then filtered off, and the filtrate was concentrated *in vacuo* and triturated with ether to afford the fully deprotected peptide amide.

Purification of the peptide was achieved by reverse-phase HPLC on a Dynamax C8 300A preparative column (21.4 × 250 mm, 5- $\mu$ m particle size) using 0.1% TFA in water as buffer A and 0.1% TFA in acetonitrile as buffer B. A linear gradient between 10% and 30% B in A over 30 min at a flow rate of 20 mL/min was used. The purified peptide was analyzed by reverse-phase HPLC on a Dynamax C8 300A analytical column (4.6 × 250 mm, 5- $\mu$ m particle size, 1 mL/min flow rate) using a variety of linear gradients between the above mentioned buffers, and it was judged to be >99% pure. The amino acid composition of the peptide was examined by amino acid analysis and was found to be consistent with the expected sequence. A sample of the purified peptide was also analyzed on a VGTOF laser desorption time-of-flight mass spectrometer at a concentration of 22 pmol/ $\mu$ L in  $\alpha$ -cyano-4-hydroxycinnamic acid, with an accelerating voltage of 22 kV. The expected molecular mass of the peptide is 2209.32 Da, and an experimental mass of 2209.2 Da was recorded.

**Size-Exclusion Chromatography.** The apparent molecular mass of the peptide was determined by size-exclusion chromatography at pH 2.5 and 6.8 using a TSK 3000SW column. Molecular mass markers used for calibrating the column were aprotinin (6.5 kDa), adrenocorticotrophic hormone (4.5 kDa), insulin A-chain (2.5 kDa), and a 22-residue synthetic peptide of lysozyme (residues 61–82) (2409 Da) which was known to be monomeric and predominantly unstructured under all the conditions studied. Columns were eluted at room temperature with 45 mM sodium phosphate buffer at a flow rate of 0.5 mL/min. Peptides were detected by absorption at 220 and 280 nm.

**Circular Dichroism Spectroscopy.** Peptide solutions were prepared by freshly dissolving the lyophilized peptide in 45 mM sodium phosphate buffer. For the experiments in which the dependence of the conformation of the peptide on the anion concentration was investigated, samples were dissolved

<sup>1</sup> Abbreviations: 2D, two dimensional; NMR, nuclear magnetic resonance; CD, circular dichroism; TFE, trifluoroethanol; ACTH, adrenocorticotrophic hormone; CCA, convex constraint analysis; MS, mass spectrometry; TFA, trifluoroacetic acid; DMF, *N,N*-dimethylformamide; Fmoc, 9-fluorenylmethoxycarbonyl; Pmc, 2,2,5,7,8-pentamethyl-6-sulfonylchroman.

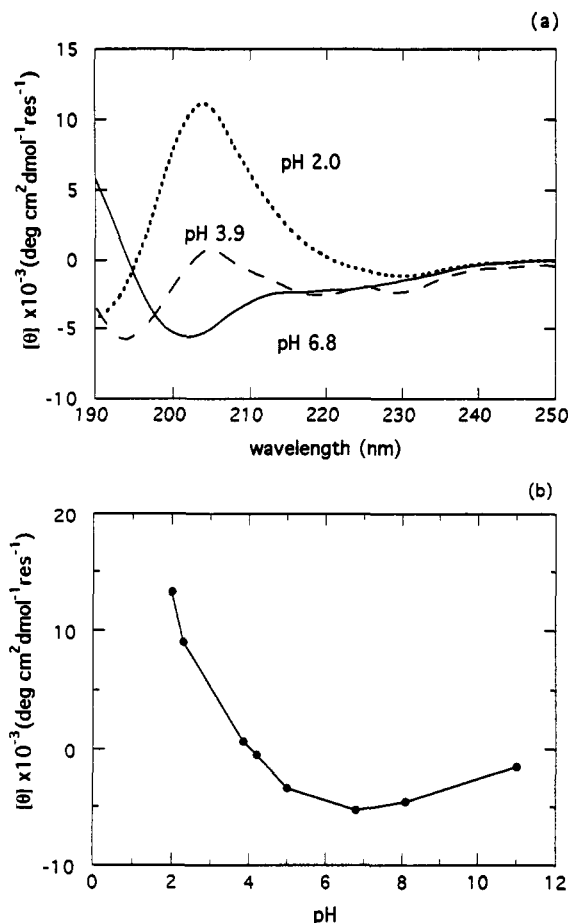


FIGURE 2: Effect of pH on the far-UV CD spectrum of the synthetic peptide. (a) CD spectra at pH 2.0 (---), pH 3.9 (- - -) and pH 6.8 (—). (b) CD signal at 204 nm as a function of pH. Spectra were obtained in 45 mM sodium phosphate buffer at 25 °C.

in  $\text{H}_2\text{O}$  at pH 2.0 or 6.8. All CD spectra were obtained with a Jasco J720 spectropolarimeter using a 1-mm quartz cell at 1.0- or 0.5-nm intervals over the wavelength range from 190 to 250 nm at 25 °C, unless otherwise stated. Molar ellipticities,  $\theta$  ( $\text{deg cm}^2 \text{ dmol}^{-1} \text{ res}^{-1}$ ), are reported. Deconvolution of the CD spectra and estimation of the secondary structural content were obtained by using convex constraint analysis (CCA) and the program LINCMB (Perczel et al., 1991).

## RESULTS

**pH Dependence.** The conformation of the peptide was examined by far-UV CD at 25 °C at pH values ranging from 2.0 to 11.2 (Figure 2). The far-UV CD spectrum of the peptide displays a remarkable pH dependence. At pH values above about 4 the spectrum is characterized by small negative maxima at 198 and 220 nm, suggesting that the peptide is predominantly unstructured under these conditions. This spectrum differs, however, from characteristic spectra of unstructured peptides and proteins, which are dominated by a large negative maximum at about 200 nm (Woody, 1985; Yang et al., 1986). This difference may result from a contribution to the spectrum of the synthetic peptide from a large positive band at 190 nm which may arise from the  $B_a$  and  $B_b$  bands of the single tyrosine residue. The magnitude of the ellipticity at 222 nm suggests that the peptide contains little (less than 6%)  $\alpha$ -helical structure (Greenfield & Fasman, 1969; Zhong & Johnson, 1992). Below pH 4 the spectrum of the peptide is quite different and is characterized by a large positive maximum at 204 nm and negative maxima at 190

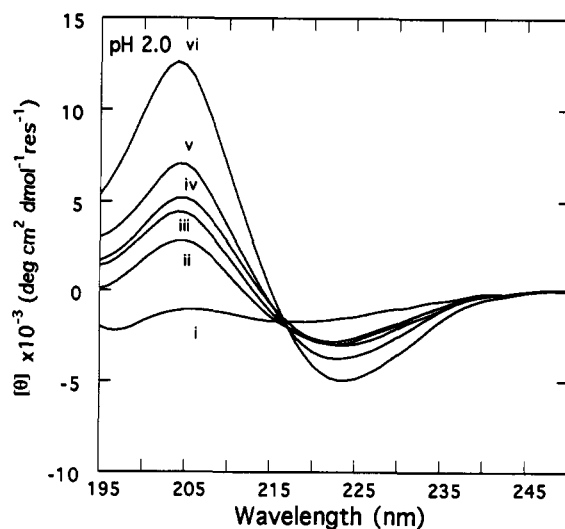


FIGURE 3: Concentration dependence of the far-UV CD spectrum of the peptide at (i) 20, (ii) 34, (iii) 46.5, (iv) 55.8, (v) 70, and (vi) 93  $\mu\text{M}$  at pH 2.0.

and 230 nm. The shape of this spectrum, particularly the location of the positive maximum at 204 nm, suggests that the peptide has adopted a substantial proportion of  $\beta$ -sheet structure at this pH, although a contribution from a type II  $\beta$ -turn, which is characterized by a weak negative maximum between 220 and 230 nm and a positive maximum between 200 and 210 nm (Woody, 1985), cannot be ruled out. Several conformations of the peptide including parallel and antiparallel  $\beta$ -sheets as well as a variety of  $\beta$ -hairpin structures are all consistent with the CD spectrum obtained. These possibilities cannot be distinguished by CD alone, and for this reason we refer to the conformation of the peptide under these conditions as " $\beta$ -structure". The intensity of the signal at 204 nm decreases dramatically when the pH is increased from 2 to 4 (Figure 2b); this transition is reversible. In the following study the properties of the peptide were examined in the  $\beta$ -conformation at pH 2.0 (low-pH form) and in the predominantly random conformation at pH 6.8 (high-pH form).

**Concentration Dependence.** The peptide was found to have only very limited solubility ( $<100 \mu\text{M}$ ), which precluded its detailed analysis by NMR spectroscopy. This also raised the possibility that the peptide is in an aggregated state in solution even at the low concentrations employed for the CD measurements. Such behavior has been well documented, particularly in the case of peptides which adopt  $\beta$ -sheet structures in solution (Hartman et al., 1974; Hilbich et al., 1991; Barrow et al., 1992). To address this issue, the concentration dependence of the far-UV CD spectrum of the peptide at pH 6.8 and 2.0 was investigated. At pH 6.8 essentially no concentration dependence of the spectrum was observed at 222 nm over the concentration range 20–93  $\mu\text{M}$ . By contrast, at pH 2.0 the spectrum obtained changed dramatically as the concentration of the peptide was reduced from 93 to 20  $\mu\text{M}$ , suggesting that structuring of the peptide at low pH involves at least some degree of intermolecular association (Figure 3). Thus, at the lowest concentration studied (20  $\mu\text{M}$ ) the spectrum resembles more closely that obtained at pH 6.8, suggesting that the peptide is predominantly unstructured, presumably containing a limited contribution from  $\beta$ -structure. At concentrations between 34 and 93  $\mu\text{M}$  a spectrum typical of the low-pH form is obtained. This transition was found to be reversible since increasing the concentration of the peptide above 20  $\mu\text{M}$  restored the spectrum typical of the  $\beta$ -structure. At the highest concentration studied (93  $\mu\text{M}$ ) visible precipitation of the peptide occurred after 9 h at 20 °C.

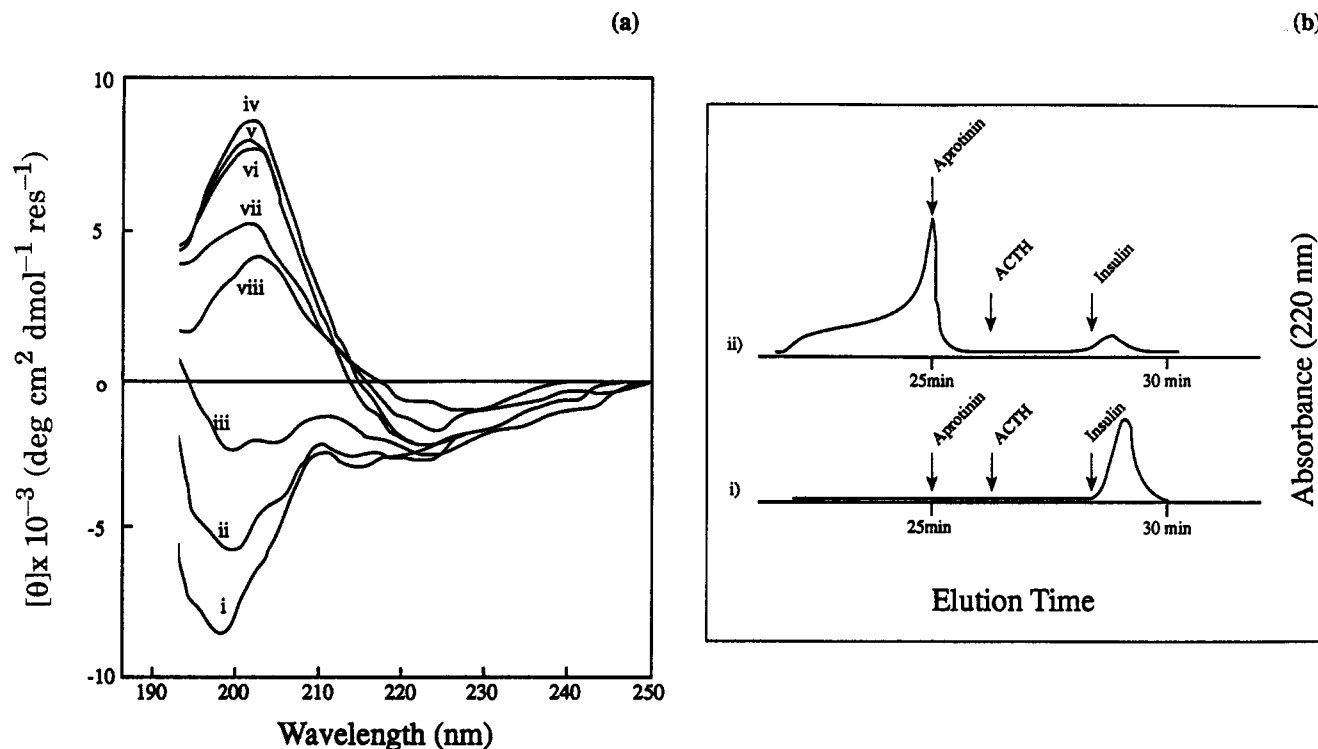


FIGURE 4: Conformation of the peptide monitored by far-UV CD and size-exclusion chromatography. Peptide (50  $\mu\text{M}$ ) was prepared in 45 mM sodium phosphate buffer at pH 6.8. The pH of the solution was then adjusted to 2.5 by the addition of  $\text{H}_3\text{PO}_4$ , and the conformation of the peptide was monitored by gel filtration chromatography and far-UV CD at different lengths of time following the acidification. (a) Far-UV CD spectra of the peptide (i) at pH 6.8 and at pH 2.5, (ii) 5 min, (iii) 3.0 h, (iv) 3.5 h, (v) 4.8 h, (vi) 6.5 h, (vii) 9.0 h, and (viii) 20.5 h after the pH was reduced. (b) Elution profiles of the peptide by gel filtration at pH 2.5 (i) 5 min and (ii) 5.0 h after the pH was reduced to 2.5.

In order to investigate this further, a second experiment was performed in which the peptide (50  $\mu\text{M}$  in 45 mM sodium phosphate buffer) was first examined at pH 6.8 by far-UV CD (Figure 4a), and the apparent molecular mass of the peptide was measured simultaneously by gel filtration chromatography in the same buffer system. As expected, the far-UV CD spectrum of the peptide at pH 6.8 was characteristic of a predominantly unstructured conformation. Gel filtration chromatography of the peptide at pH 6.8, however, displayed the presence of two distinct peaks, both of which have apparent molecular masses (3000 and 2500 Da) close to that calculated from the amino acid sequence of the peptide (2209 Da), but significantly smaller than that predicted for a dimeric species. Considering that the far-UV CD spectrum is concentration independent over this range at this pH, these species most probably represent monomeric forms of the peptide which elute anomalously on the column. The pH of the solution was then reduced from pH 6.8 to 2.5, and the far-UV CD spectrum and the apparent molecular mass of the peptide were measured as quickly as possible (5 min) and at various lengths of time after the pH jump. Five minutes after the acidification, the overall shape of the CD spectrum was unperturbed relative to that of the high-pH form, although a decrease in the magnitude of the ellipticity at 198 nm was observed. For this sample a single species was observed by gel filtration, with an apparent molecular mass (2090 Da) close to that of the monomeric form (Figure 4b, trace i). After 4.8 h at pH 2.5 a spectrum typical of the low-pH form had evolved, and as judged by gel filtration, the peptide had adopted predominantly trimeric and higher oligomeric states. At times exceeding 4.8 h, the magnitude of the ellipticity at 204 nm began to decrease and the peptide had formed only higher oligomeric forms as judged by gel filtration. It is clear, therefore, that decreasing the pH from 6.8 to 2.5 results in

a slow conversion of the peptide from a presumably monomeric and predominantly unstructured state to a mixture of higher oligomeric forms which occurs concomitantly with the formation of  $\beta$ -structure as judged by far-UV CD. In this latter form the solubility of the peptide is significantly decreased, which ultimately results in precipitation of the peptide and a decrease in the magnitude of the CD signal at 204 nm. Interestingly, when the pH of the solution was raised to pH 6.8, rapid (within minutes) conversion of the oligomeric, low-pH form to the monomeric, predominantly random, high-pH form occurred. This shows that, although the transition is reversible, the kinetics of interconversion of the two states is very different. For this reason care was taken in the following experiments to ensure as far as possible that the concentrations and ages of the samples prepared at pH 2.0 were identical.

**Temperature Dependence.** The stability of the conformations of the two pH forms of the peptide was measured as a function of temperature between 2 and 65  $^{\circ}\text{C}$ . There is virtually no temperature dependence of the far-UV CD spectrum at pH 6.8 over the entire temperature range studied (data not shown). By contrast, at pH 2.0 a dramatic temperature dependence is observed (Figure 5). First, as the temperature is raised from 2 to 20  $^{\circ}\text{C}$ , the molar ellipticity at 204 nm is increased. Above approx. 30  $^{\circ}\text{C}$  this signal then decreases dramatically until at approx. 55  $^{\circ}\text{C}$  a spectrum resembling closely that of a predominantly unstructured state characteristic of the high-pH form of the peptide is observed. Analysis of this species by gel filtration confirmed that it had adopted the monomeric form at this temperature. The cooperative nature of this transition is in marked contrast to the more usual linear temperature dependence typically observed for structured peptides of this size in aqueous solution (Barrow et al., 1992) presumably as a consequence of the intermolecular interactions in the low-pH form of the peptide.

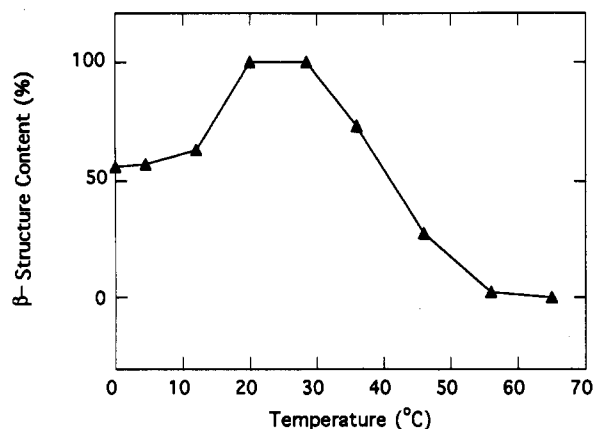


FIGURE 5: Temperature dependence of the  $\beta$ -conformation of the low-pH form of the peptide at pH 2.0. The data have been normalized to the ellipticity at 204 nm at 20 °C, which is given a value of 100%.

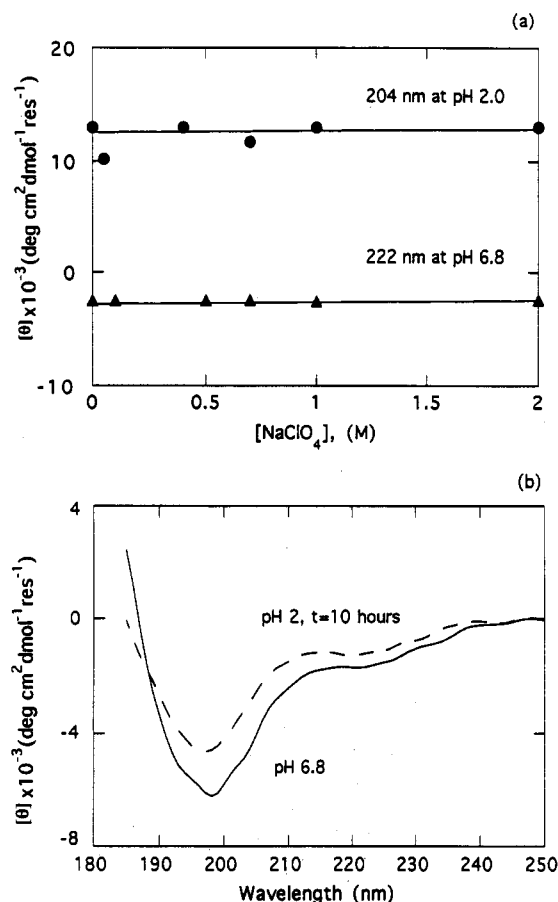


FIGURE 6: (a) Dependence of the conformation of the low-pH form at 204 nm (●) and of the high-pH form of the peptide at 222 nm (▲) at different ionic strengths. (b) Effect of ionic strength on the transition of the high-pH form to the low-pH form of the peptide. Peptide (30  $\mu$ M) at pH 6.8 in 2.0 M NaClO<sub>4</sub> (—) was acidified to pH 2.0, and spectra were acquired at different times after the acidification. The spectrum 10 h after the pH jump is shown (---).

When the sample was cooled from 55 to 20 °C, a spectrum resembling that of the low-pH form of the peptide was again produced, although it was reduced in intensity relative to that of the sample before heating. Thus, the transition appears to be only partially reversible under these conditions.

**Ionic Strength.** The addition of NaClO<sub>4</sub> up to a concentration of 2.0 M has no observable effect on the conformation of the peptide in both the high- and low-pH forms (Figure 6a). Similarly, adding Na<sub>2</sub>SO<sub>4</sub> to the same final ionic strength (0.67 M) has no effect on the far-UV CD spectra of both

forms of the peptide. Gel filtration of the low- and high-pH forms of the peptide in the presence of 0.67 M Na<sub>2</sub>SO<sub>4</sub> confirmed that the oligomeric state of the low-pH form was maintained at this high ionic strength and that the high-pH form of the peptide at high ionic strength is monomeric. Thus, maintenance of the conformation of the low-pH form is presumably independent of electrostatic effects over the range studied. Interestingly, however, although increasing the ionic strength has no observable effect on the associated low-pH form of the peptide, it has a dramatic effect on the initial oligomerization process. Thus, when the high-pH form of the peptide (34  $\mu$ M in 2.0 M NaClO<sub>4</sub>, pH 6.8) was acidified to pH 2.0, a relatively stable form of the peptide was obtained, the far-UV CD spectrum of which did not change over a period of 10 h and which resembled closely that of the original high-pH form (Figure 6b). Clearly, therefore, the low-pH form of the peptide in the presence of 2.0 M NaClO<sub>4</sub> is a relatively stable, predominantly random structure. Intermolecular association, which is required for formation of  $\beta$ -structure, is therefore retarded significantly in the presence of high concentrations of NaClO<sub>4</sub>. In order to test this more thoroughly, the experiment was repeated, but this time the high-pH form of the peptide was diluted into pH 2.0 buffer containing 0.67 M Na<sub>2</sub>SO<sub>4</sub>. In this case a spectrum typical of the low-pH form of the peptide was obtained *more* rapidly than in the experiment at low ionic strength. This indicates that the slow rate of association of the peptide to form  $\beta$ -structure in NaClO<sub>4</sub> is not merely an effect of the high ionic strength, but presumably specific binding of the perchlorate anions to the peptide. In addition, the known effect of sulfate anions to stabilize protein structures more than perchlorate anions, increasing hydrophobic interactions, may be responsible for the rapid formation of  $\beta$ -structure in 0.67 M Na<sub>2</sub>SO<sub>4</sub> (Collins & Washabaugh, 1985).

**Effects of TFE and Methanol.** (i) *The High-pH Form.* Organic solvents such as TFE and methanol are known to promote the formation of secondary structure in peptides and proteins (Shibata et al., 1992; Sönnichsen et al., 1992). It has been suggested that this is due, at least in part, to the highly hydrophilic nature of the backbone peptide unit, which is effectively reduced in low-dielectric solvents (Sönnichsen et al., 1992). TFE has been found to stabilize helices in peptide fragments corresponding to helical regions in native proteins and in protein fragments predicted to have significant helical propensity (Segawa et al., 1991; Dyson et al., 1992a; Shin et al., 1993). By contrast, formation of  $\beta$ -sheet structure in TFE is less common, but has also been reported (Toniolo et al., 1979). The effect of TFE on the far-UV CD spectrum of the peptide in the high- and low-pH forms, therefore, was investigated.

The high-pH form of the peptide shows a large increase in the magnitude of the ellipticity at 222 and 206 nm upon the addition of TFE (Figure 7a). The observation of an isodichroic point at 204 nm suggests that there is an equilibrium between two distinct conformations of the peptide in TFE. Analysis of these spectra using the convex constraint analysis (CCA) algorithm of Fasman (Perczel et al., 1991) confirms that the spectra may be deconvoluted into two pure components, one representing a predominantly disordered structure akin to that of the high-pH form of the peptide in aqueous solution (component I) and the other (component II) is at least partially  $\alpha$ -helical in nature (Figure 7b). Fitting these spectra using three pure components did not result in a significant decrease in the error. As judged by the magnitude of the ellipticity at 222 nm, a helical content, on average, of about 20% is obtained

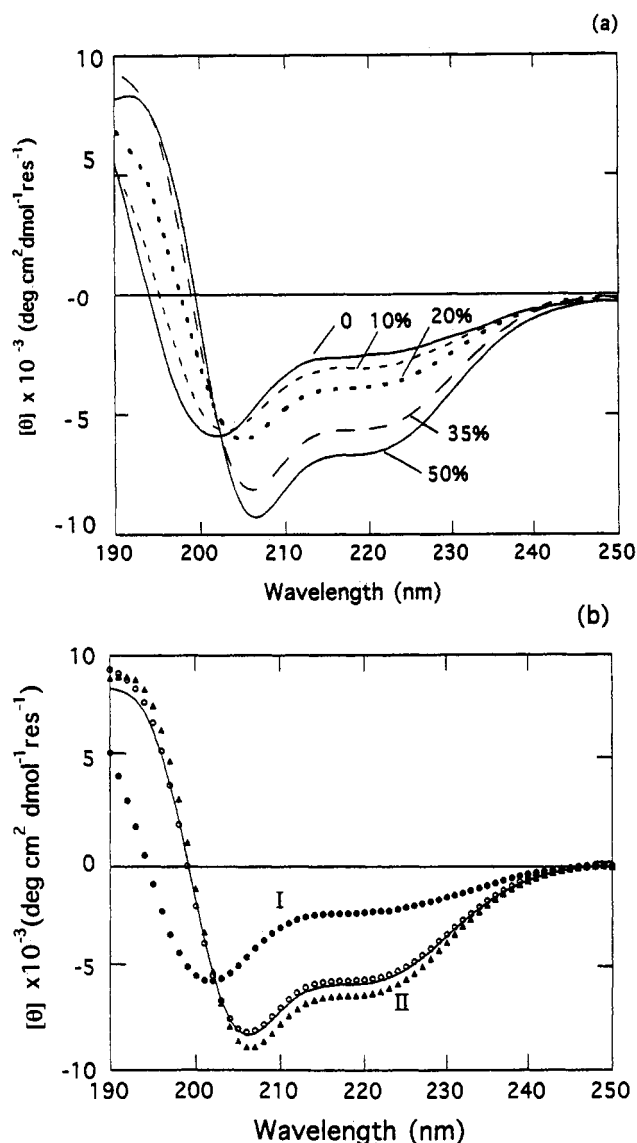


FIGURE 7: Effect of TFE on the conformation of the high-pH form of the peptide. (a) Far-UV CD spectra of the peptide in the presence of 0, 10%, 20%, 35%, and 50% (v/v) TFE. (b) Two-component convex constraint deconvolution (Perczel et al., 1991) of the CD curves in (a). The two components are shown [(●) component I; (▲) component II] as well as the experimental curve in the presence of 35% (v/v) TFE (○) and the estimated fitted curve (—).

in 50% (v/v) TFE (Zhong & Johnson, 1992). Taking the length dependence of the ellipticity for an  $\alpha$ -helix into account, however, suggests that the actual helical content may be higher than this (Gans et al., 1991). Methanol, although showing an effect similar to that of TFE, is significantly less potent; in this case a helical content of about 12% as judged by the method of Zhong and Johnson (1992) is induced in 50% (v/v) methanol (not shown).

(ii) *The Low-pH Form.* The effect of TFE on the far-UV CD spectrum of the low-pH form of the peptide is shown in Figure 8a. By contrast to the previous situation, this transition is complex and at least three distinct events are observed. First, at concentrations of TFE up to approx. 10% (v/v) the magnitude of the molar ellipticity at 204 nm increases. In the second phase (between 10 and 20% (v/v) TFE), the molar ellipticity is reduced with a concomitant blue shift in the positive maximum to about 201 nm. Finally, at TFE concentrations exceeding 20% (v/v), a dramatic change in the spectrum is observed and a spectrum resembling closely that of the helical form of the peptide in 50% (v/v) TFE at

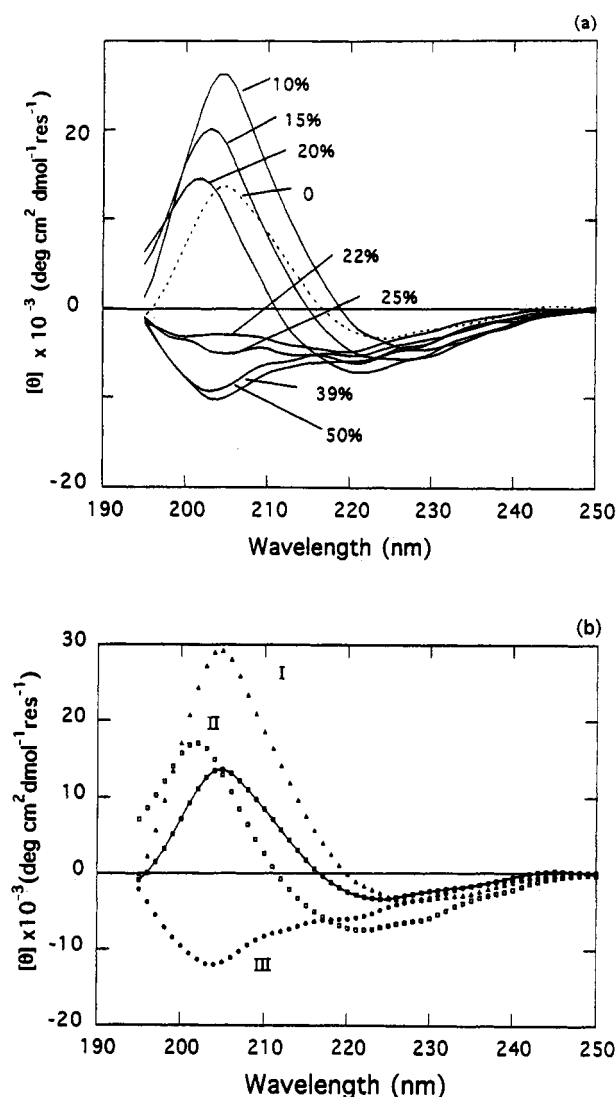


FIGURE 8: Effect of TFE on the conformation of the low-pH form of the peptide in 45 mM sodium phosphate buffer at 25 °C. (a) Far-UV CD spectra of the peptide in the presence of 0, 10%, 15%, 20%, 22%, 25%, 39%, and 50% (v/v) TFE. (b) Three-component convex constraint deconvolution of the CD curves in (a). The three pure components' spectra are shown: (▲) component I, (□) component II, and (●) component III. The experimental curve in the presence of 0% (v/v) TFE (■) and the estimated fitted curve (—) are also displayed.

pH 6.8 is formed. Analysis of the latter species by gel filtration showed that the oligomeric  $\beta$ -structure had been disrupted and that the species in 50% (v/v) TFE was monomeric in nature. Consistent with this, deconvolution of these spectra using the program CCA (Perczel et al., 1991) required at least three pure components to obtain an adequate fit (Figure 8b). The spectrum of component I resembles closely that of the low-pH form of the peptide in aqueous solution; that of component II also resembles the spectrum expected for a predominantly  $\beta$ -conformation, although this differs from the spectrum of component I in that the wavelength of the positive maximum is shifted to 201 nm and the molar ellipticity of the negative maximum at 221 nm is larger than that of component I. The third component resembles more closely that of the helical form of the peptide in 50% (v/v) TFE. Clearly, an intermediate with a distinct conformation as judged by this technique is populated during the transition. It is possible that this represents reorganization of the  $\beta$ -structure prior to its denaturation at higher concentrations of TFE. In the presence of 50% (v/v) TFE, an average  $\alpha$ -helical content of

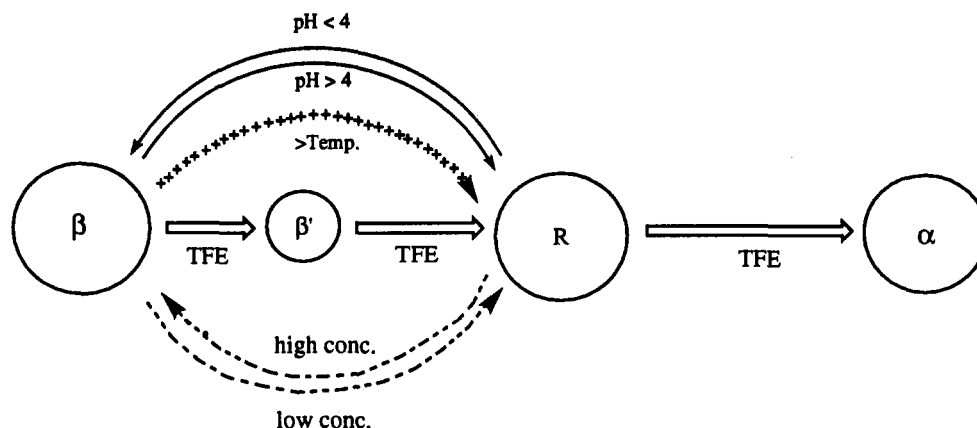


FIGURE 9: Schematic diagram of the different conformational states of the peptide populated under different solution conditions: ( $\beta$ )  $\beta$ -structure; (R) predominantly unstructured state; and ( $\alpha$ ) state containing, on average,  $\sim 20\%$   $\alpha$ -helical structure. The  $\beta'$ -state is formed at low concentrations of TFE at low pH and represents an intermediate state populated during the denaturation of the  $\beta$ -state with TFE. The different states are distinguished by their characteristic far-UV CD spectra (see text). Due to the concentration dependence of the conformation of the low-pH form of the peptide, the reversibility of the titration with TFE was not assessed. For this reason the reaction is shown as unidirectional in the direction of increasing TFE concentration.

about 18% is estimated by the method of Zhong and Johnson (1992) and about 16% as judged by the CCA algorithm. By contrast to the above, methanol shows virtually no effect on the conformation of the peptide at pH 2.0 under these conditions (not shown).

## DISCUSSION

Investigation of the conformation of the peptide fragment of hen egg white lysozyme which forms a triple-stranded  $\beta$ -sheet in the native protein has revealed several important features of the conformational preferences of this sequence which may be of importance in understanding the formation of  $\beta$ -sheet structures in general and which may be relevant to our understanding the folding behavior of the intact protein. The most striking result is that at least three distinct conformations of the peptide are observed under different solution conditions (Figure 9). First, at pH values below 4.0 the far-UV CD spectrum of the peptide is dominated by a large positive maximum at 204 nm, and it is tempting to suggest, therefore, that the peptide forms  $\beta$ -sheet structure at this pH (denoted here as the  $\beta$ -state). This structure is associated with the formation of trimers and higher oligomeric forms of the peptide. One outstanding question in this work is the precise nature of the structure induced. By far-UV CD alone the origin of the CD signal cannot be uniquely defined. Conformations including both parallel and antiparallel  $\beta$ -strands as well as  $\beta$ -hairpin structures are all consistent with the spectrum obtained. What is clear from this work, however, is that intermolecular interactions are required to stabilize this structure, suggesting that extended  $\beta$ -strands from different peptide molecules interact to form the putative  $\beta$ -sheet structure. The large positive maximum at 204 nm is red shifted from the theoretical value between 195 and 200 nm calculated for a regular antiparallel  $\beta$ -sheet, suggesting that the structure induced may be twisted from an ideal planar arrangement of strands (Manning et al., 1988). It is interesting to note that the  $\beta$ -sheet in the native state of hen lysozyme is also significantly distorted in the X-ray and solution structures (Handoll, 1985; Smith et al., 1993), although the relationship between the structure in the multimeric peptide and in the intact monomeric protein molecule is difficult to judge. At pH values above 4.0 a second conformation of the peptide which is predominantly random in nature is observed (denoted here as the R-state). This state has less than 6% helical character as judged by the magnitude of the ellipticity

at 222 nm. This is in accord with earlier studies of the conformation of a proteolytic fragment of hen lysozyme encompassing residues 45–61 which is also predominantly unstructured at pH 6.8 (Segawa et al., 1991). The third conformational state (the  $\alpha$ -state) involves  $\alpha$ -helical structure and is observed at both low and high pH in the presence of TFE and at high pH in methanolic solution. In this state, at concentrations of 50% (v/v) TFE, on average about 20%  $\alpha$ -helical structure is induced as judged by the magnitude of the molar ellipticity at 222 nm. Interestingly, secondary structure prediction based on a variety of methods (Chou & Fasman, 1978; Garnier et al., 1978; Kyte & Doolittle, 1982) suggests that the  $\alpha$ -helical propensity inherent in this sequence is low relative to that in the helical regions in the native protein, although a weak propensity for  $\alpha$ -helical structure is apparent in the first and third strands as judged by the method of O'Neil and DeGrado (1990). Thus, even though TFE and methanol can promote the formation of  $\alpha$ -helical structure in this peptide, the solvents are much less effective than observed with peptide fragments arising from  $\alpha$ -helical regions in native lysozyme (K. Bolin, D. Raleigh, M. Pitkeathly, and C. M. Dobson, unpublished results) and in other proteins (Dyson et al., 1992a; Shin et al., 1993). Indeed,  $\alpha$ -helical structure is induced along virtually the entire length of a synthetic peptide from the C-helix of hen lysozyme under conditions very similar to those used here (K. Bolin, D. Raleigh, M. Pitkeathly, and C. M. Dobson, unpublished results).

The dramatic pH dependence of the peptide conformation suggests that the ionization state of the side chains of the peptide may play an important role in the conformational switch. Thus, at pH values below 4.0 only the single Arg residue is charged. By contrast, at pH values greater than 4.0 the two Asp residues are presumably also charged, resulting in both an increase in the number of charged groups and a change in the net charge on the peptide from +1 to -1. It is possible that the relatively high local charge density involving the two charged Asp side chains at pH 6.8 prevents the formation of  $\beta$ -structure in the synthetic peptide by disrupting the intermolecular interactions required for its formation. The electrostatic effect cannot be the only effect involved in the pH-dependent conformational change of the peptide, however, since perchlorate or sulfate anions, which have high affinity for the peptide cation, have little effect on the conformation of the peptide in the high-pH form. The inability to shield the charge effect at pH 6.8 by high ionic strength indicates

that the ionization state of the side chains does not make a major contribution to the conformational switch. Hydrophobicity of the side chains and the inherent  $\beta$ -sheet propensity of the amino acid sequence presumably also play essential roles in determining the conformation of the peptide. It is interesting in this regard that mutation of only a single residue (Ile56 to Thr) in the  $\beta$ -sheet of human lysozyme results in the precipitation of the full-length protein molecule in amyloid fibrils (Pepys et al., 1993). This highlights the importance of understanding the mechanism of  $\beta$ -sheet formation in terms not only of the determinants of protein folding but also of the maintenance of these structures in the cellular environment.

The effect of TFE and methanol on the conformation of the low-pH form of the peptide, remarkably, is quite different. First, although concentrations of methanol up to 50% (v/v) have no apparent effect on the conformation of the peptide at low pH, in the presence of TFE the conformational transition is complex and involves an intermediate state with a novel far-UV CD spectrum (denoted the  $\beta'$  state in Figure 9). The CD spectrum (in which the positive maximum occurs at 201 nm) of this intermediate resembles closely that predicted for a planar antiparallel  $\beta$ -sheet (Manning et al., 1988), suggesting that reorganization of an apparently distorted  $\beta$ -sheet structure may occur at low concentrations of TFE. This is followed, at higher concentrations of the organic solvent, by denaturation of the structure to a predominantly monomeric random conformation which contains, on average, about 20%  $\alpha$ -helical structure.

In our previous studies, a stable partially folded state of lysozyme was observed in 50% (v/v) TFE at pH 2.0. This state is characterized by a substantially reduced near-UV CD signal and a dramatic increase in the ellipticity in the far-UV CD, such that the magnitude of the ellipticity is apparently 2-fold greater than that of the native protein (Buck et al., 1993). In more recent studies we have shown that TFE also has a similar effect on the structure of lysozyme at pH 6.8, but in this case the transition from the native state to the TFE state occurs at higher TFE concentrations (H. Lu, M. Buck, and C. M. Dobson, unpublished data). The structural features responsible for the apparent excess ellipticity in the far-UV CD have not been determined, although several possibilities exist, including formation of novel helical structure not found in the native protein, extension or reorganization of existing helical structure, or rearrangement of aromatic residues and/or disulfide bonds which also contribute to this spectral region (Woody, 1985; Siligardi et al., 1992; Chakrabartty et al., 1993). Examination of this state by NMR revealed, however, that only the native-like  $\alpha$ -helical elements are sufficiently stable for the amides involved to be protected from hydrogen exchange (Buck et al., 1993). The result of the study on the synthetic peptide described here suggests that part of the apparent excess ellipticity in the TFE state of lysozyme could arise from conversion of the  $\beta$ -sheet region in the intact protein to novel  $\alpha$ -helical structure. Assuming, however, that the extent of  $\alpha$ -helix formation induced in the  $\beta$ -sheet region of the native protein is at least similar to that formed in the synthetic peptide, this clearly cannot make a major contribution to the ellipticity of the TFE state. The possibility remains, therefore, that other regions of the  $\beta$ -domain including the long loop or the  $3^{10}$  helix perhaps coupled with extension of the native helices in the  $\alpha$ -domain may contribute this effect.

The structural transition of the peptide from a putative  $\beta$ -sheet conformation at low pH to a predominantly random structure at neutral pH and to partial  $\alpha$ -helical structure in the presence of TFE and methanol shows that the environment

of a given amino acid sequence is very important in determining the nature of the secondary structure formed. These results are not specific to the sequence studied here; indeed, in peptide fragments of other proteins, as well as in several intact proteins,  $\beta$ -sheet to  $\alpha$ -helical transitions have been reported to be induced or enhanced by changing the solvent conditions (Greenfield & Fasman, 1969; Bello, 1988; Hilbich et al., 1991; Barrow et al., 1992; Zhong & Johnson, 1992; Fan et al., 1993). This may well be of relevance to the early steps in protein folding, since solvent exclusion in early collapsed states may generate environments which promote secondary structure formation to different extents in different peptide sequences (Dobson et al., 1994). For sequences that have low intrinsic preference for a particular type of secondary structure the possibility exists, therefore, that the structure formed may be very sensitive to the precise nature of the collapsed state, and this may account for the apparent complexity of folding pathways observed for many proteins (Dobson et al., 1994). If this is the case, these sequences may undergo dramatic conformational changes early during the folding pathway. Studies of peptide fragments of putative folding regions should help to throw light on this important issue.

A striking feature of the kinetic folding pathway of hen lysozyme is that, at least in the majority of molecules, the  $\beta$ -domain is unable to fold to a stable entity able to protect amides significantly from hydrogen exchange in the absence of a stable, structured  $\alpha$ -domain. In addition, formation of the  $\beta$ -domain is one of the slowest events observed in the folding pathway (Radford et al., 1992; Miranker et al., 1993). Despite this, reconstruction of the far-UV CD spectrum of the folding intermediates formed after only 4 ms suggest that a native-like complement of secondary structure is already formed by this time (Chaffotte et al., 1992). Although it is difficult to correlate the results obtained with a 20-residue peptide fragment, structuring of which requires intermolecular association at low pH, with folding of the monomeric protein, which has been studied in detail at pH 5.2 (Radford et al., 1992), it is interesting nonetheless to speculate on the significance of these results for the folding of the intact enzyme. Formation of the presumably  $\beta$ -sheet structure in the peptide requires intermolecular association at low pH, and at pH 6.8 this structure could not be formed at all under the variety of conditions investigated here. By contrast, the conformation of the intact protein is unchanged from pH 7 to 2, although the protein is less stable at low pH (Imoto et al., 1972). This suggests that support from a stable structured  $\alpha$ -domain may be a fundamental requirement for folding of the  $\beta$ -domain to a stable entity in the folding pathway of the enzyme. Further dissection of the lysozyme molecule into putatively independent folding units may reveal further insight into the role of individual interactions in directing the protein folding pathway.

#### ACKNOWLEDGMENT

We thank G. Fasman for generously providing the CCA program, A. Maisey of VG Analytical for mass spectral analysis of the peptide, T. Willis and P. Lawson for performing the amino acid analyses, S. Cole for help with size-exclusion chromatography, J. Seelig et al. for sending us a preprint of their manuscript, L. Smith and M. O. Berners for help with the graphics, and A. Drake and A. Rodger for helpful discussion. We are very grateful for the support and advice of C. M. Dobson during the course of this work, and we thank him for critically reading the manuscript prior to publication.

## REFERENCES

- Ananthanarayanan, V. S., Chan, N., & Yang, D. S. C. (1993) *Biochem. Cell Biol.* 71, 236–240.
- Barrow, C., Yasuda, A., Kenny, P. T. M., & Zagorski, M. (1992) *J. Mol. Biol.* 225, 1075–1093.
- Bello, J. (1988) *Biopolymers* 27, 1627–1640.
- Blake, C. C. F., Koenig, D. F., Mair, G. A., & Sarma, R. (1965) *Nature* 206, 757–761.
- Blanco, F. J., Jimenez, M. A., Rico, M., Santoro, M., Herranz, J., & Nieto, J. L. (1991) *Eur. J. Biochem.* 200, 345–351.
- Brown, J. E., & Klee, W. A. (1971) *Biochemistry* 10, 470–476.
- Buck, M., Radford, S. E., & Dobson, C. M. (1993) *Biochemistry* 32, 669–678.
- Chaffotte, A. F., Guillou, Y., & Goldberg, M. E. (1992) *Biochemistry* 31, 9694–9702.
- Chakrabartty, A., Kortemme, T., Padmanabhan, S., & Baldwin, R. L. (1993) *Biochemistry* 32, 5560–5565.
- Chou, P. Y., & Fasman, G. D. (1978) *Adv. Enzymol.* 47, 45–148.
- Collins, K. D., & Washabaugh, M. W. (1985) *Q. Rev. Biophys.* 18, 323–422.
- Cox, J. P. L., Evans, P. A., Packman, L. C., Williams, D. H., & Woolfson, D. N. (1993) *J. Mol. Biol.* 234, 483–492.
- Dobson, C. M. (1992) *Curr. Opin. Struct. Biol.* 2, 6–12.
- Dobson, C. M., Evans, P. A., & Radford, S. E. (1994) *Trends Biochem. Sci.* 19, 31–37.
- Dyson, H. J., Merutka, G., Waltho, J. P., Lerner, R. A., & Wright, P. E. (1992a) *J. Mol. Biol.* 226, 795–817.
- Dyson, H. J., Sayre, J., Merutka, G., Shin, H.-C., Lerner, R. A., & Wright, P. E. (1992b) *J. Mol. Biol.* 226, 819–835.
- Evans, P. A., & Radford, S. E. (1994) *Curr. Opin. Struct. Biol.* 4, 100–107.
- Fan, P., Bracken, C., & Baum, J. (1993) *Biochemistry* 32, 1573–1582.
- Gans, P. J., Manning, M. C., Woody, R. W., & Kallenbach, N. R. (1991) *Biopolymers* 31, 1605–1614.
- Garnier, J., Osguthorpe, D. J., & Robson, B. (1978) *J. Mol. Biol.* 120, 97–120.
- Goodman, E. M., & Kim, P. S. (1989) *Biochemistry* 28, 4343–4347.
- Greenfield, N., & Fasman, G. D. (1969) *Biochemistry* 8, 4108–4116.
- Handoll, H. H. G. (1985) D. Phil. Thesis, University of Oxford.
- Hartman, R., Schwaner, R. C., & Hermans, J. (1974) *J. Mol. Biol.* 90, 415–429.
- Haynie, D. T., & Friere, E. (1993) *Proteins* 16, 115–140.
- Hilbich, C., Kisters-Woike, B., Reed, J., Masters, C. L., & Beyreuther, K. (1991) *J. Mol. Biol.* 218, 149–163.
- Imoto, T., Johnson, L. N., North, A. C. T., Phillips, D. C., & Rupley, J. A. (1972) *The enzymes* (Boyer, P. D., Ed.) 3rd ed., Vol. 7, pp 665–867, Academic Press, New York.
- Kraulis, P. (1991) *J. Appl. Crystallogr.* 24, 946–950.
- Kyte, J., & Doolittle, R. F. (1982) *J. Mol. Biol.* 157, 105–132.
- Manning, M. C., Illangasekare, M., & Woody, R. W. (1988) *Biophys. Chem.* 31, 77–86.
- Marqusee, S., & Baldwin, R. L. (1987) *Proc. Natl. Acad. Sci. U.S.A.* 84, 8898–8902.
- McCammon, J. A., Northrup, S. H., Karplus, M., & Levy, R. M. (1980) *Biopolymers* 19, 2033–2045.
- Miranker, A., Robinson, C. V., Radford, S. E., Alpin, R. T., & Dobson, C. M. (1993) *Science* 262, 896–900.
- Oas, T. G., & Kim, P. S. (1988) *Nature* 336, 42–48.
- O'Neil, K. T., & DeGrado, W. F. (1990) *Science* 250, 646–651.
- Pepys, M. B., Hawkins, P. N., Booth, D. R., Vigushin, D. M., Tennent, G. A., Soutar, A. K., Totty, N., Nguyen, O., Blake, C. C. F., Terry, C. J., Feest, T. G., Zalin, A. M., & Hsuan, J. J. (1993) *Nature* 362, 553–556.
- Perczel, A., Hollósi, M., Tusnády, G., & Fasman, G. D. (1991) *Protein Eng.* 4, 669–679.
- Radford, S. E., Dobson, C. M., & Evans, P. A. (1992) *Nature* 358, 302–307.
- Segawa, S.-S., Fukuno, T., Fujiwara, K., & Noda, Y. (1991) *Biopolymers* 31, 497–509.
- Shibata, A., Yamamoto, M., Yamashita, T. Y., Chiou, J.-S., Kamaya, H., & Ueda, I. (1992) *Biochemistry* 31, 5728–5733.
- Siligardi, G., Campbell, M. M., Gibbons, W. A., & Drake, A. F. (1992) *Eur. J. Biochem.* 206, 23–29.
- Shin, H.-C., Merutka, G., Waltho, J. P., Tennant, L. L., Dyson, H. J., & Wright, P. E. (1993) *Biochemistry* 32, 6356–6364.
- Shoemaker, K. R., Kim, P. S., York, E. J., Stewart, J. M., & Baldwin, R. L. (1987) *Nature* 326, 563–567.
- Sönnichsen, F. D., Van Eyk, J. E., Hodges, R. S., & Sykes, B. D. (1992) *Biochemistry* 31, 8790–8798.
- Smith, L. J., Sutcliffe, M. J., Redfield, C., & Dobson, C. M. (1993) *J. Mol. Biol.* 229, 930–944.
- Terzi, E., Holzemann, G., & Seelig, J. (1994) *Biochemistry* 33, 1345–1350.
- Tessari, M., Foffani, M. T., Mammi, S., & Peggion, E. (1993) *Biopolymers* 33, 1877–1887.
- Toniolo, C., Bonora, G. M., Salardi, S., & Mutter, M. (1979) *Macromolecules* 12, 620–625.
- Woody, R. W. (1985) *Peptides* 7, 15–114.
- Wu, L. C., Laub, P. B., Elöve, G. A., Carey, J., & Roder, H. (1993) *Biochemistry* 32, 10271–10276.
- Yang, J. T., Wu, C.-S., & Martinez, H. M. (1986) *Methods Enzymol.* 130, 208–269.
- Yapa, K., Weaver, D. L., & Karplus, M. (1992) *Proteins* 12, 237–265.
- Zhong, L., & Johnson, W. C., Jr. (1992) *Proc. Natl. Acad. Sci. U.S.A.* 89, 4462–4465.